

Extremely Stretchable Electroluminescent Devices with Ionic Conductors

Jiangxin Wang, Chaoyi Yan, Guofa Cai, Mengqi Cui, Alice Lee-Sie Eh, and Pooi See Lee*

Stretchable electronics are emerging as a new type of devices with their excellent mechanical compliance compared to the rigid or flexible devices. They can confront demanding mechanical deformations such as flexing, twisting, stretching, folding, or conformably wrapping, enabling electronic applications under rigorous mechanical conditions that cannot be addressed with conventional devices. As a type of “soft” electronics, stretchable electroluminescent (EL) devices drive special interest and are believed to be essential technologies for the next generation lighting and display applications.^[1–11] Their soft physical form will initiate plenty of unprecedented applications such as biomedical related applications which use implantable devices on curvilinear tissue surfaces, 3D displays which render contents physically, and interactive visual systems which provide users tactile interaction besides visual information, etc. The stretching conditions in these applications may require the EL devices to confront reversible deformations beyond 100% strains, which are beyond the capability of most of the demonstrated stretchable EL devices.^[1,6,9,12,13] Superelastic EL devices are yet to be explored with significantly improved mechanical properties and functionalities. Stretchable conductor is an important component in realizing deformable EL devices. Stretchable conductors with thick and opaque structures, such as buckled metal films,^[4,5] carbon nanotube paste,^[1] and arranged nickel composites^[9] have been demonstrated as electrical interconnects to assemble rigid devices for stretchable light-emitting systems. To apply the stretchable conductors as electrodes for stretchable light-emitting devices, thin and transparent electrode structures are required for efficient light extraction, such as 1D nanomaterials networks,^[13,14] transferred graphene films on elastomer,^[8,15] hybrid of 1D and 2D nanomaterials,^[16,17] and buckled poly(3,4-ethylenedioxythiophene):poly(styrenesulfonate) (PEDOT:PSS) thin films.^[6,18] The emissive layer is another critical part in the stretchable EL devices. Light-emitting diodes (LEDs) and light-emitting electrochemical cells (LEECs) operate under low voltages (<10 V) and large injection current (typically >10 mA cm⁻²) for light emission. Stable conductivity in the stretchable and transparent electrode is required to maintain the current in these

devices under stretching conditions, which is still challenging to resolve.^[13,19,20] On the contrary, we have demonstrated in our previous study that alternating-current electroluminescent (ACEL) devices operate under high voltage with low dependence on the stretchable and transparent electrodes.^[21] The unique emission mechanism in the ACEL devices with promising advantages for stretchable EL devices will be further exploited in this study.

In order to fabricate the stretchable electrodes, two different strategies, with one focusing on stretchable structures and the other focusing on stretchable materials, have been explored.^[22] Due to the daunting materials challenges in stretchable electronic conductors, the structural tailoring strategy has been widely practiced to develop stretchable electrodes for deformable EL devices. For example, Kim et al. patterned thin metal films into stretchable structures and used them as electrical interconnects to assemble rigid light-emitting elements on elastic substrates.^[3–5] Conventional technologies could be combined to enable stretchable electronics with the approach. However, large-scale and cost-effective techniques need to be developed to manipulate the stretchable structures and to assemble components with significant mechanical mismatches for durable deformable devices. Furthermore, since the metal films are opaque, these electrodes are not suitable for stretchable EL devices which require good transmittance for efficient light extraction. Recently, carbon nanotubes (CNTs) and silver nanowires (AgNWs) have been demonstrated as highly conductive fillers in polymer matrix to achieve transparent and stretchable electrodes with their percolating network structure.^[19,23–25] Combining with stretchable emissive layers, the transparent and stretchable electrodes could be used to achieve fully stretchable EL devices.^[13,21] Although stretchable devices at high strains can be achieved, it is still quite challenging to extend the stretching limits of these nanomaterial networks beyond 100% due to damage on the thin network structures under large mechanical deformations.

Compared to the stretchable electronic conducting structures, which need to circumvent difficulties in their stretchability, mechanical stability, and transmittance, the intrinsically stretchable ionic conductors can be easily formed with solid polymer host, yielding extraordinary mechanical properties and transparency.^[26–28] They have been demonstrated as promising materials for soft actuators,^[29,30] strain sensors,^[31,32] transistors,^[33,34] etc. Here, we report the demonstration of extremely stretchable EL devices using ionic conductors as the stretchable, deformable, and transparent conducting electrodes. Limited by the stretchability in the precedent transparent electronic conductors, the ACEL devices could only be stretched to 100%.^[21] In this study, we demonstrate that ionic conductors

J. X. Wang, Dr. C. Y. Yan,^[†] Dr. G. F. Cai, M. Q. Cui, A. L.-S. Eh, Prof. P. S. Lee
School of Materials Science and Engineering
50 Nanyang Avenue
Nanyang Technological University
Singapore 639798, Singapore
E-mail: pslee@ntu.edu.sg



^[†]Present address: School of Advanced Materials, Peking University Shenzhen Graduate School, Shenzhen, 518055.

DOI: 10.1002/adma.201504187

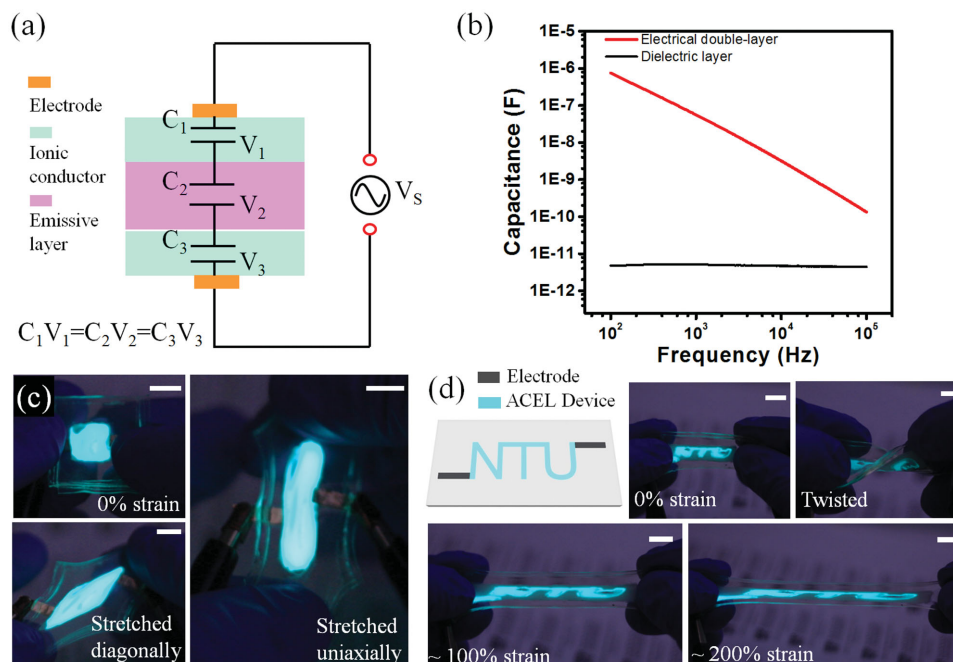


Figure 1. a) Schematic representation of the ACEL device using ionic conductor. The equivalent circuit of the EL device shows three capacitors connected in series. b) Capacitance of the electrical double layer and emissive layer under different frequencies. c) Photographs of the ACEL devices stretched diagonally or uniaxially. d) A schematic image of the patterned device and photographs of the patterned device under twist or stretch. Scale bars in (c) and (d) are 10 mm.

lead to breakthrough in the stretchability and transparency of the electrodes for ACEL devices. The stretchable ACEL devices with ionic conductors can confront extreme mechanical deformations with stretching strains up to 700%.

Figure 1a shows a schematic illustration of the extremely stretchable ACEL device. The device is composed of the bottom and top ionic conductors with sandwiched ZnS:Cu/Ecoflex emissive layer. The working mechanism of ionic conductors has been reported by Suo and co-workers.^[26] In brief, the alternating current was capacitively coupled to the device through three capacitors connected in series, as shown in the equivalent circuit in Figure 1a. Capacitors C_1 and C_3 were formed by the electrical double layers at the ionic conductor/external electrode interfaces on each side of the device. The emissive ZnS:Cu/Ecoflex composite constituted the capacitor C_2 . Electrochemical stability is a key consideration when the ionic conductors are applied in devices which operate under high voltage. Especially, the ACEL devices generally require 100–1000 V for light emission. Depending on the electrode materials, the electrochemical stability window for the lithium based polycarbonate electrolyte is around 3 V.^[35] In the electrical double layer, due to the small charge separation (in the range of a few nm), they have large capacitance on the order of $\approx 10^{-1}$ F m⁻². On the contrary, the dielectric capacitor in the emissive layers of ACEL devices with polymer binders have significantly larger charge separation (around 200 μ m), leading to much smaller capacitance on the order of $\approx 10^{-7}$ F m⁻².^[26] C_2 is much smaller compared to C_1 or C_3 (C_2/C_1 or $C_2/C_3 = \approx 10^{-5}$ – 10^{-4} in the frequency range of 100–1000 Hz), as shown in Figure 1b. With all the capacitors connected in series, one can obtain $C_1V_1 = C_2V_2 = C_3V_3$ as the charges stored in each capacitor are the same. Thus, it can be

derived that most of the voltage will be coupled onto the emissive layer with small voltage distributed on the double layer interfaces ($\approx 10^{-2}$ – 10^{-1} V for ACEL device operate at 1000 V) due to their much larger capacitance. As shown in Figure 1b,c, light emission could be achieved in the ACEL devices using ionic conductor as the highly stretchable electrodes. The device can be stretched uniaxially, elongated diagonally, and twisted. The ionic conductors and emissive layers can be easily deposited with solution-processable methods. They can be patterned into different device geometrics. As shown in Figure 1c, the stretchable ACEL device was patterned. The patterned device could operate under highly stretched states.

Ionic conductors are interesting for their extremely high transmittance and stretchability compared to conventional electronic conductors. As illustrated in **Figure 2a**, the prepared ionic conductors in a 50 mL bottle shows excellent transparency. A thin layer of ionic conductor (≈ 200 μ m in thickness) was coated on a glass slide, Figure 2a (right). Transparency of the ionic conductor was measured with another glass slide as reference. As presented in Figure 2b, transmittance of the ionic conductor almost reaches 100% (beyond the photometric accuracy, $\pm 0.3\%$, of the Shimadzu UV-2500pc spectrometer) in the wavelength range of 350–850 nm. To study the electrical properties and stretchability of the ionic conductor, a 200 μ m thick ionic conductor was coated on a 3M VHB tape with two graphite electrodes used as external connections, as illustrated in Figure 2c. The ionic conductor was tested under stretching strains up to 700%, as shown in Figure 2d. As well known, resistance of a conductor can be given by $R = \rho L/A$, where R , ρ , L , and A are the resistance, resistivity, length, and cross-section area of the conductor ($\rho = 1780$ Ω cm). The resistivity test on the

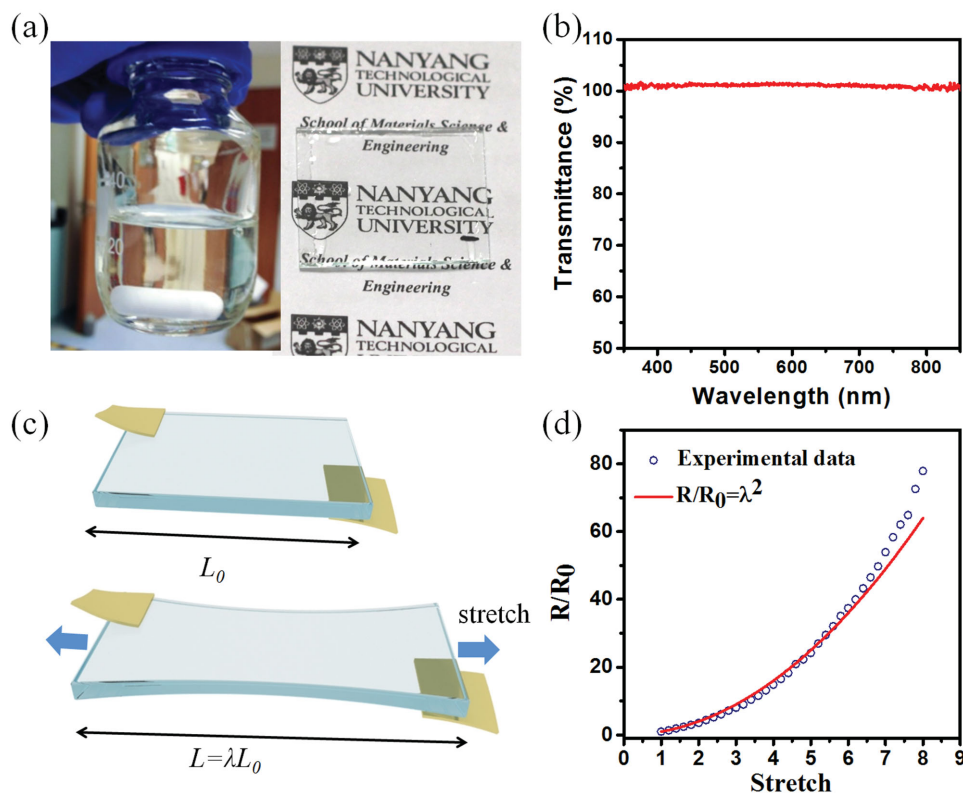


Figure 2. a) Photographs of the as-prepared ionic conductor in a glass bottle (left) and ionic conductor coated on a glass slide with a thickness of $\approx 200 \mu\text{m}$ (right). b) Transmittance spectrum of the ionic conductor on glass slide. Another glass slide was used as reference. c) A schematic image of the ionic conductor under stretching test. d) Resistance change of the ionic conductor measured as a function of the stretching strains.

ionic conductor was carried out by the electrochemical impedance spectroscopy (EIS), Figure S1, Supporting Information). Under the stretch ratio of λ , $R = \lambda^2 R_0 \rho / \rho_0$ ($L/A = \lambda^2 L_0 / A_0$). The ionic conductor is considered as incompressible. R_0 , ρ_0 , L_0 , and A_0 are resistance, length, and cross-section area of the conductor in the unstretched state).^[26] Resistance change of the conductor closely matches with the $R/R_0 = \lambda^2$ curve with the stretch ratios below 6, indicating that the resistivity of the ionic conductor is independent with the stretch ratio. The resistance change is above the $R/R_0 = \lambda^2$ curve with the stretch ratios beyond 6, indicating that the resistivity of the ionic conductor may have slightly increased. The stretchability and mechanical stability of the ionic conductors significantly exceed that of the known transparent electronic conductors. For example, resistance of the stretchable and transparent AgNWs embedded in elastomers increased 20–35 times at the strains of 100%.^[7,19,20] Resistance in CNT film embedded in elastomer changed more than eight times at the strains of 120%.^[36,37] In addition, the significantly deteriorated conductivity under repeated deformations is another critical problem in these electrodes.^[7,19,20,36] On the contrary, the ionic gel easily accommodates the mechanical deformations and maintain constant resistance after recovered from the stretch. Resistance of the ionic conductor rarely changes after repetitively stretched to 700% for 1000 cycles, as shown in Figure S2 (Supporting Information). Though conductivity of the ionic conductors is still lower compared to the electronic conductors, they are suitable for electronic components

such as the ACEL devices in which the conductivity requirement can be easily met.

Stretchable ACEL devices have been demonstrated with AgNWs film embedded in PDMS as the stretchable transparent conductors with limited stretchability at 100%.^[21] Utilizing the extremely stretchable and transparent ionic conductor, we demonstrate that stretchability of the ACEL devices can be significantly improved. As shown in Figure 3a, the ACEL devices could be elongated up to 700% with maintained device operation. The excellent stretchability in the ACEL device exceeds all the demonstrated EL devices with stretchable emission components.^[6,7,13,21,24,38] Figure 3b shows the emission performance of the extremely stretchable ACEL devices before stretch. The maximum luminance of the stretchable ACEL device could reach $\approx 95 \text{ cd m}^{-2}$, which might be suitable for indoor applications with the luminance requirement of $100\text{--}200 \text{ cd m}^{-2}$.^[6,39,40] Further improvement in the device brightness could be achieved with improvement in the conductivity of the ionic conductors and dielectric constant of the emissive layer. Luminance of the ACEL device was plotted against the electrical field under the frequency of 2 kHz. Emission brightness and the applied voltage on the ACEL devices follow the relation of $L = L_0 \exp(-\beta/V^{1/2})$, where L is the luminance, V is the applied voltage, and L_0 and β are the constants decided by the devices.^[41] The experimental data fit well with the relation (Figure 3b), the root-mean-square deviation of the fitting is ≈ 0.94 , which was preserved under different strains

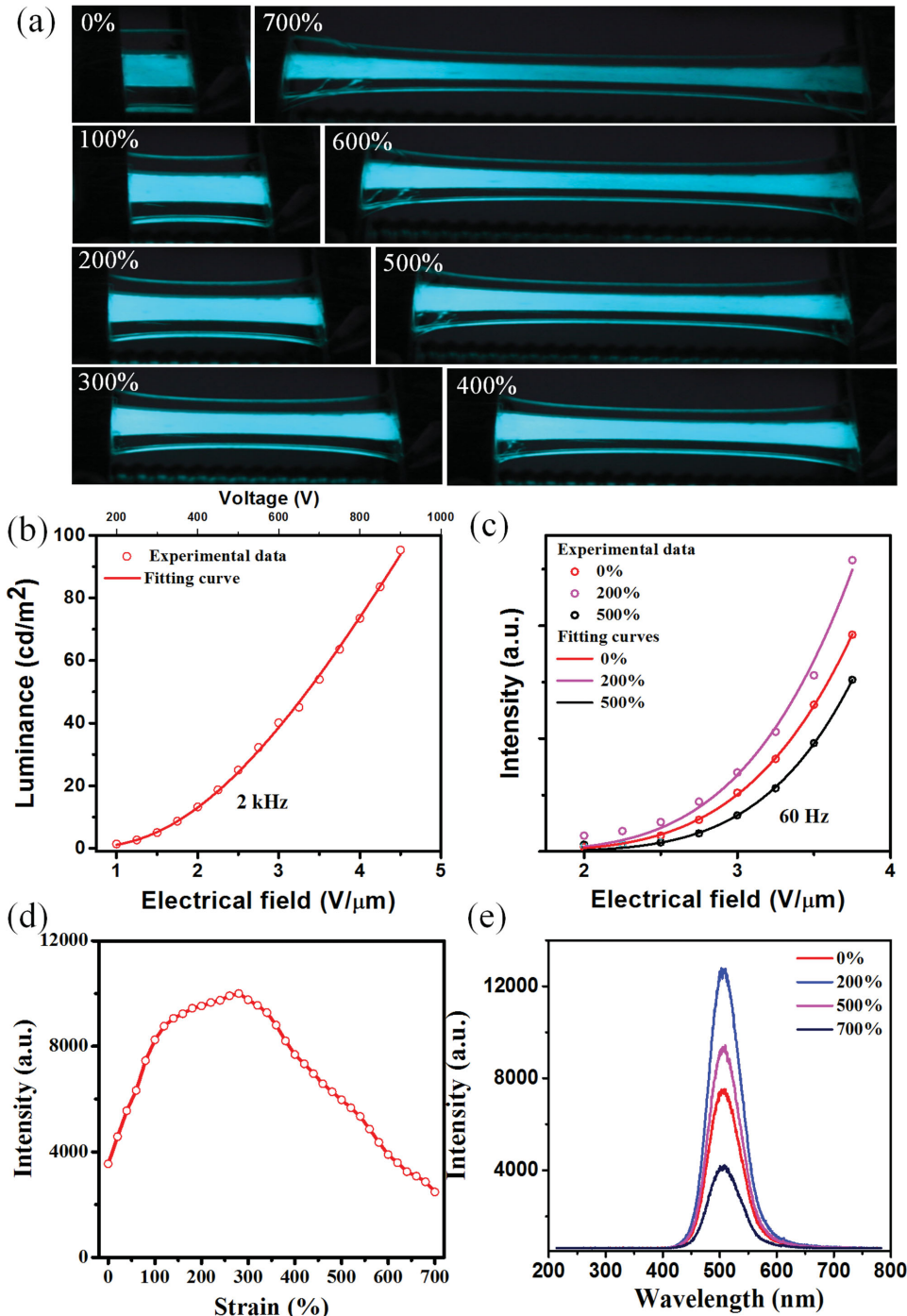


Figure 3. a) Photographs of the EL device stretched to different strains. b) Luminance–electrical field characteristic of the stretchable ACEL device under 0% strain. c) Luminance–electrical field characteristics of the ACEL device under different strains. d) Emission intensity of the EL device under different stretching strains. e) Electroluminescent spectrum of the elastic EL device at the stretching strains of 0%, 200%, 500%, and 700%.

(Figure 3c) with varied L_0 and β . The relation between the emission brightness and applied voltage leads to unique behavior of the device under strains. The emission performance was examined when the device was stretched to different states under constant bias. As shown in Figure 3d, emission intensity of the stretchable EL device first increased with the stretching strains

and reached the maximum value at 280% ($I_{280}/I_0 = 282\%$, I_{280} and I_0 are the emission intensity at 280% and 0% strains, respectively). The emission intensity began to decrease after the strains exceeded 280%. Emission intensity at 700% strains still maintained at about 70% of the emission intensity at 0% strain (original unstrained state). Emission spectra of the device

remained unchanged under strains, as shown in Figure 3e. All the emission spectra center at 506 nm with the full width at half-maximum (FWHM) of 67 nm. Variation of the emission intensity of the stretchable EL device under different strains can be understood by the brightness–voltage relation with combined effects of reduced emissive layer thickness and increased device area under increased strains. Reducing the film thickness leads to increase in the electrical field in the emissive layer (contribute to increase device brightness) while increasing the device area leads to declined phosphor density in the polymer matrix (contribute to reduce device brightness). Though the capacitance of the emissive layer will also change under stretch, it is still relatively small compared to the capacitance of the electrical double layer. Voltage on the emissive layer will not be significantly affected under stretch (detail discussion is provided in the Supporting Information). Relation of the emission film thickness and phosphor density to the device luminance was reported in stretchable ACEL devices using AgNWs as the transparent electrode.^[21] Different from the previous work on AgNWs, which showed slight increase in the emission intensity before the strains of 30% with subsequent decrease in the intensity under larger strains, the intensity was observed to increase until the strains reached 280% in the ACEL devices with ionic conductors. First of all, it is believed that the largely varied network structure in the AgNW films, which was used as the stretchable and transparent conductor in the previous report play an important role in the emission intensity reduction under strains. With the network structure, light transmittance takes place through the open regions. The electrical field will be focused around the nanowires with decreased field intensity in the open regions away from the nanowires. Under increasing strains, the area of the open regions will increase with further decreased electrical field in these regions, resulting in the emission intensity loss in the devices. Though the transparent AgNWs electrode has large resistance variation under stretch,^[19] it is relatively small compared to the resistance in the emissive layer and thus not playing a major role in reducing the device luminance. Detail discussion on the effect of resistance change in the AgNWs and ionic conductor under stretch is provided in the Supporting Information. Unlike the AgNW network, ionic conductors can fully cover the surface of the

emission layer under different strains. Besides, the resistance in the ionic conductors may become comparable to the resistance of the emissive layer, contributing to the change in current and affect the luminance of the stretchable ACEL devices. With differences in the structure and resistance in the ionic conductor, luminance change in the ACEL devices with ionic conductors also behaved differently from the device with AgNW electrodes.

Cycling stability of the stretchable EL device was also investigated. The highly stretchable ACEL device was stretched between 40% and 400% (a video was provided in the Supporting Information to demonstrate the extremely stretchable ACEL and its cycling stability test). As it requires a relatively long time (a couple of hours) for the highly strained device to fully recover to the initial state, the device was only allowed to relax at 40% to reduce the testing time. The stretching speed for the cycle test is 10 mm s^{-1} , corresponding to a strain rate of $\approx 71\% \text{ s}^{-1}$ with the original device length of 14 mm. **Figure 4a** shows the stretching test of the device in 25 cycles. I_{400}/I_{40} varied between 1.66 and 2.01, where I_{400} and I_{40} are the brightness of the device under stretching strains of 400% and 40%, respectively. The variation might be contributed to the change in the strained states due to the mechanical hysteresis in the highly strained polymer. **Figure 4b** shows that performance of the device is quite stable under the cycling test compared to previous fully stretchable EL devices.^[13,21] Emission intensity of the device maintained at $\approx 85\%$ after stretched to 400% for 1000 cycles. The emission fluctuation in the initial stretch–relaxation cycles was attributed to the contact problem between the electrode and electrolyte during the measurement.

In conclusion, ionic conductors are studied as innovative electrodes for ACEL devices. The ionic conductors deliver outstanding features of extremely high stretchability and transmittance compared to the conventional electronic electrodes. The ionic conductors were prepared with simple blending processes and could be easily deposited onto arbitrary substrates with different methods such as spin-coating,^[42,43] screen printing,^[44,45] inkjet printing,^[46,47] etc. The demonstrated idea expands the research scope of the electrode materials for ACEL devices, benefiting either the conventional rigid and planar devices or the new emerging “soft” devices. With the high stretchability

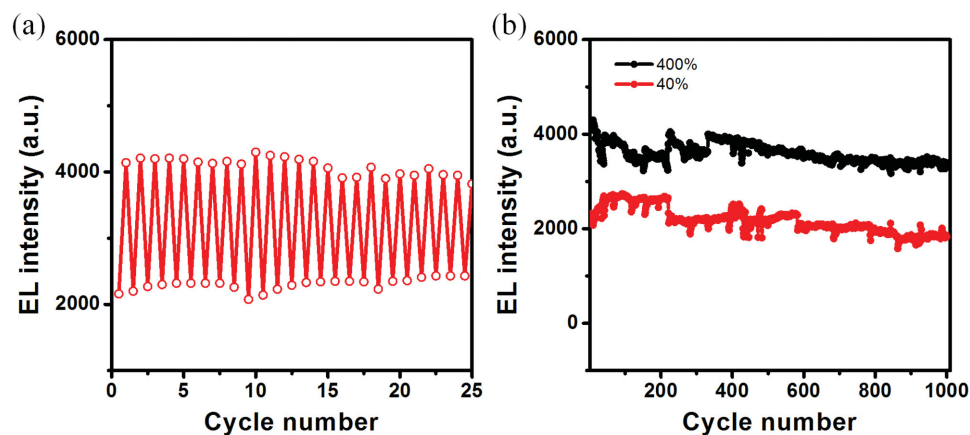


Figure 4. a) Cycling stability of the device in 25 cycles. b) Mechanical stability test of the device with 1000 cycles.

in the ionic conductor, an extremely stretchable ACEL device was reported with a stretchability of 700%. Unique emission behavior of the stretchable ACEL devices was observed with increased emission intensity at stretching strains below 280% and decreased emission intensity at larger tensile strains. At 700% strain, brightness of the device still maintained at 70% of the initial emission intensity at 0% strain. The extremely stretchable ACEL device also exceeded all the preceding works. Its excellent mechanical stability allows it to be repetitively stretched to 400% with fairly stable device performance. The presented extremely stretchable EL devices provide new opportunities in stretchable lightings, volumetric 3D displays, interactive readout systems, and other unprecedented applications.

Experimental Section

Preparation of Ionic Conductor: Poly(methyl methacrylate) (PMMA, average $M_w = \approx 350\,000$), lithium perchlorate (LiClO_4), propylene carbonate (PC), and acetonitrile were purchased from Sigma-Aldrich and used as received. 0.75 g of LiClO_4 was first dissolved in 2 g of PC. After the LiClO_4 was fully dissolved, 7.86 g of acetonitrile was mixed with the solution. 1.5 g of PMMA was slowly added into the blended solution and stirred at 1000 rpm overnight. Viscous and clear gel-like solution was obtained after the PMMA was fully dissolved.

Fabrication of the Highly Stretchable ACEL Devices with Ionic Conductors: The ionic gel prepared as described above was deposited onto a 3M VHB tape (thickness of 1 mm) with the thickness of $\approx 100\ \mu\text{m}$ by doctor-blade coating. The ionic conductor was then dried in an oven for 6 h at $60\ ^\circ\text{C}$ to allow the acetonitrile to be fully evaporated, leading to a solid polymer film for subsequent layer deposition. A commercial available silicone elastomer, Ecoflex 00-50 was used as the polymer matrix to enable high stretchability in the emissive layer. The silicone elastomer was prepared with one part Ecoflex 00-50 A and one part Ecoflex 00-50 B (Smooth-On). ZnS:Cu microparticles (Shanghai KPT company, SEM image of the ZnS:Cu particles was shown in Figure S4, Supporting Information) were mixed with the Ecoflex solution in the weight ratio of 1:1. The prepared ZnS:Cu/Ecoflex composite was then coated on the ionic conductor by doctor-blade coating with the thickness controlled at $\approx 200\ \mu\text{m}$. The composite was allowed to cure under room temperature for 2 h. Another ionic gel layer in the thickness of $\approx 100\ \mu\text{m}$ was subsequently coated as the top electrode. Copper tape or graphite paper was used to electrically connect the ionic conductors with the external power source. VHB tape with the thickness of 0.5 mm was laminated on top to seal the whole device structure and complete the device fabrications. Patterning on the device was achieved by using shadow mask with the designed pattern during the coating of bottom and top electrode. The device fabrication procedures were the same as described above.

Device Characterization: The transmittance spectra were measured by a Shimadzu spectrometer (UV-2501pc). Resistance of the ionic conductors under stretching test was measured by an Agilent E4980A precision LCR meter with an amplitude of 50 mV and a frequency of 1 kHz in room temperature ($\approx 25\ ^\circ\text{C}$). Capacitance of the electrical double layer and emissive layer was measured with an HP 4194 impedance analyzer which provided the frequency measurement range of 100 Hz to 40 MHz. Stretching test of the sample was performed on a home-made motorized linear translation stage in room temperature. A function generator (Yokogawa FG 300) connected with a power amplifier (Trek PZD 2000) was used to apply alternating voltage for the highly stretchable ACEL devices. Emission from the device was collected by an optical fiber connected to an Acton SP-2300 monochromator. Emission spectra from the devices were measured by a Princeton Pixis 100B spectroscopy CCD detector on the monochromator. Luminance of the devices was measured by a Konica CS-200 spectroradiometer.

Supporting Information

Supporting Information is available from the Wiley Online Library or from the author.

Acknowledgements

The authors thank V. Kumar, V. Bhavanasri, and Dr. S. H. Li for discussion on the electrochemical characterizations. This work was supported by the National Research Foundation Competitive Research Programme, Award No. NRF-CRP-13-2014-02. J.X.W. would like to acknowledge the scholarship awarded by the Nanyang Technological University, Singapore.

Received: August 27, 2015

Revised: October 19, 2015

Published online: December 4, 2015

- [1] T. Sekitani, H. Nakajima, H. Maeda, T. Fukushima, T. Aida, K. Hata, T. Someya, *Nat. Mater.* **2009**, *8*, 494.
- [2] C. Wang, D. Hwang, Z. B. Yu, K. Takei, J. Park, T. Chen, B. W. Ma, A. Javey, *Nat. Mater.* **2013**, *12*, 899.
- [3] S. I. Park, Y. Xiong, R. H. Kim, P. Elvikis, M. Meitl, D. H. Kim, J. Wu, J. Yoon, C. J. Yu, Z. Liu, Y. Huang, K. C. Hwang, P. Ferreira, X. Li, K. Choquette, J. A. Rogers, *Science* **2009**, *325*, 977.
- [4] R. H. Kim, D. H. Kim, J. L. Xiao, B. H. Kim, S. I. Park, B. Panilaitis, R. Ghaffari, J. M. Yao, M. Li, Z. J. Liu, V. Malyarchuk, D. G. Kim, A. P. Le, R. G. Nuzzo, D. L. Kaplan, F. G. Omenetto, Y. G. Huang, Z. Kang, J. A. Rogers, *Nat. Mater.* **2010**, *9*, 929.
- [5] X. L. Hu, P. Krull, B. de Graff, K. Dowling, J. A. Rogers, W. J. Arora, *Adv. Mater.* **2011**, *23*, 2933.
- [6] M. S. White, M. Kaltenbrunner, E. D. Glowacki, K. Gutnichenko, G. Kettlgruber, I. Graz, S. Aazou, C. Ulbricht, D. A. M. Egbe, M. C. Miron, Z. Major, M. C. Scharber, T. Sekitani, T. Someya, S. Bauer, N. S. Sariciftci, *Nat. Photonics* **2013**, *7*, 811.
- [7] J. J. Liang, L. Li, K. Tong, Z. Ren, W. Hu, X. F. Niu, Y. S. Chen, Q. B. Pei, *ACS Nano* **2014**, *8*, 1590.
- [8] R. H. Kim, M. H. Bae, D. G. Kim, H. Y. Cheng, B. H. Kim, D. H. Kim, M. Li, J. Wu, F. Du, H. S. Kim, S. Kim, D. Estrada, S. W. Hong, Y. G. Huang, E. Pop, J. A. Rogers, *Nano Lett.* **2011**, *11*, 3881.
- [9] S. Kim, J. Byun, S. Choi, D. Kim, T. Kim, S. Chung, Y. Hong, *Adv. Mater.* **2014**, *26*, 3094.
- [10] H. L. Filiatrault, G. C. Porteous, R. S. Carmichael, G. J. E. Davidson, T. B. Carmichael, *Adv. Mater.* **2012**, *24*, 2673.
- [11] M. Vosgueritchian, J. B. H. Tok, Z. N. Bao, *Nat. Photonics* **2013**, *7*, 769.
- [12] J. Wang, C. Yan, K. J. Chee, P. S. Lee, *Adv. Mater.* **2015**, *27*, 2876.
- [13] J. J. Liang, L. Li, X. F. Niu, Z. B. Yu, Q. B. Pei, *Nat. Photonics* **2013**, *7*, 817.
- [14] Z. B. Yu, X. F. Niu, Z. T. Liu, Q. B. Pei, *Adv. Mater.* **2011**, *23*, 3989.
- [15] K. S. Kim, Y. Zhao, H. Jang, S. Y. Lee, J. M. Kim, K. S. Kim, J. H. Ahn, P. Kim, J. Y. Choi, B. H. Hong, *Nature* **2009**, *457*, 706.
- [16] M. S. Lee, K. Lee, S. Y. Kim, H. Lee, J. Park, K. H. Choi, H. K. Kim, D. G. Kim, D. Y. Lee, S. Nam, J. U. Park, *Nano Lett.* **2013**, *13*, 2814.
- [17] B. W. An, B. G. Hyun, S. Y. Kim, M. Kim, M. S. Lee, K. Lee, J. B. Koo, H. Y. Chu, B. S. Bae, J. U. Park, *Nano Lett.* **2014**, *14*, 6322.
- [18] M. Vosgueritchian, D. J. Lipomi, Z. N. Bao, *Adv. Funct. Mater.* **2012**, *22*, 421.
- [19] J. Wang, C. Yan, W. Kang, P. S. Lee, *Nanoscale* **2014**, *6*, 10734.
- [20] W. L. Hu, X. F. Niu, L. Li, S. R. Yun, Z. B. Yu, Q. B. Pei, *Nanotechnology* **2012**, *23*, 344002.
- [21] J. Wang, C. Yan, K. J. Chee, P. S. Lee, *Adv. Mater.* **2015**, *27*, 2876.

- [22] Y. G. Sun, Y. D. Yin, B. T. Mayers, T. Herricks, Y. N. Xia, *Chem. Mater.* **2002**, *14*, 4736.
- [23] C. Feng, K. Liu, J. S. Wu, L. Liu, J. S. Cheng, Y. Y. Zhang, Y. H. Sun, Q. Q. Li, S. S. Fan, K. L. Jiang, *Adv. Funct. Mater.* **2010**, *20*, 885.
- [24] C. H. Liao, C. W. Huang, J. Y. Chen, C. H. Chiu, T. C. Tsai, K. C. Lu, M. Y. Lu, W. W. Wu, *J. Phys. Chem. C* **2014**, *118*, 8194.
- [25] X. Y. Zeng, Q. K. Zhang, R. M. Yu, C. Z. Lu, *Adv. Mater.* **2010**, *22*, 4484.
- [26] C. Keplinger, J. Y. Sun, C. C. Foo, P. Rothmund, G. M. Whitesides, Z. G. Suo, *Science* **2013**, *341*, 984.
- [27] B. H. Chen, J. J. Lu, C. H. Yang, J. H. Yang, J. X. Zhou, Y. M. Chen, Z. G. Suo, *ACS Appl. Mater. Interfaces* **2014**, *6*, 7840.
- [28] B. H. Chen, Y. Y. Bai, F. Xiang, J. Y. Sun, Y. M. Chen, H. Wang, J. X. Zhou, Z. G. Suo, *J. Polym. Sci., Part B: Polym. Phys.* **2014**, *52*, 1055.
- [29] M. Shahinpoor, *Electrochim. Acta* **2003**, *48*, 2343.
- [30] J. A. Rogers, *Science* **2013**, *341*, 968.
- [31] J. Y. Sun, C. Keplinger, G. M. Whitesides, Z. G. Suo, *Adv. Mater.* **2014**, *26*, 7608.
- [32] A. Frutiger, J. T. Muth, D. M. Vogt, Y. Menguc, A. Campo, A. D. Valentine, C. J. Walsh, J. A. Lewis, *Adv. Mater.* **2015**, *27*, 2440.
- [33] J. H. Cho, J. Lee, Y. Xia, B. Kim, Y. Y. He, M. J. Renn, T. P. Lodge, C. D. Frisbie, *Nat. Mater.* **2008**, *7*, 900.
- [34] K. H. Lee, M. S. Kang, S. P. Zhang, Y. Y. Gu, T. P. Lodge, C. D. Frisbie, *Adv. Mater.* **2012**, *24*, 4457.
- [35] B. Sun, J. Mindemark, K. Edstrom, D. Brandell, *Solid State Ionics* **2014**, *262*, 738.
- [36] L. B. Hu, W. Yuan, P. Brochu, G. Gruner, Q. B. Pei, *Appl. Phys. Lett.* **2009**, *94*, 161108.
- [37] T. Chen, H. S. Peng, M. Durstock, L. M. Dai, *Sci. Rep.* **2014**, *4*, 3612.
- [38] J. V. van de Groep, P. Spinelli, A. Polman, *Nano Lett.* **2012**, *12*, 3138.
- [39] B. Hekmatshoar, A. Z. Kattamis, K. H. Cherenack, K. Long, J. Z. Chen, S. Wagner, J. C. Sturm, K. Rajan, M. Hack, *IEEE Electron Device Lett.* **2008**, *29*, 63.
- [40] S. Steudel, K. Myny, S. Schols, P. Vicca, S. Smout, A. Tripathi, B. van der Putten, J. L. van der Steen, M. van Neer, F. Schutze, O. R. Hild, E. van Veenendaal, P. van Lieshout, M. van Mil, J. Genoe, G. Gelinck, P. Heremans, *Org. Electron.* **2012**, *13*, 1729.
- [41] D. R. Vij, *Handbook of Electroluminescent Materials, Series in Optics and Optoelectronics*, IOP, Bristol, UK **2004**.
- [42] K. H. Lee, S. P. Zhang, T. P. Lodge, C. D. Frisbie, *J. Phys. Chem. B* **2011**, *115*, 3315.
- [43] V. Narasimhan, S. Y. Park, *Langmuir* **2015**, *31*, 8512.
- [44] P. Gan, J. S. Foord, R. G. Compton, *Electroanalysis* **2014**, *26*, 1886.
- [45] Z. Tehrani, T. Korochkina, S. Govindarajan, D. J. Thomas, J. O'Mahony, J. Kettle, T. C. Claypole, D. T. Gethin, *Org. Electron.* **2015**, *26*, 386.
- [46] S. Limem, P. Calvert, *J. Mater. Chem. B* **2015**, *3*, 4569.
- [47] U. Loffelmann, N. Wang, D. Mager, P. J. Smith, J. G. Korvink, *J. Polym. Sci., Part B: Polym. Phys.* **2012**, *50*, 38.